Journal of Applied Mechanics and Technical Physics, Vol. 50, No. 2, pp. 318–326, 2009

PROCESSES OF HYDRATE FORMATION AND DISSOLUTION BEHIND A SHOCK WAVE IN A LIQUID CONTAINING GAS BUBBLES (MIXTURE OF NITROGEN AND CARBON DIOXIDE)

V. E. Dontsov, V. E. Nakoryakov, and E. V. Dontsov

UDC 532.529

The processes of dissolution and hydrate formation behind a moderate-amplitude shock wave in water containing gas bubbles (mixture of nitrogen and carbon dioxide) are studied in experiments with different initial static pressures in the medium and concentrations of carbon dioxide in bubbles. An increase in static pressure in the gas–liquid medium is demonstrated to enhance the influence of the non-reacting gas (nitrogen) on the processes of dissolution and hydrate formation.

Key words: *shock wave, liquid, gas bubbles, bubble fragmentation, dissolution, hydrate formation.*

One of the most important factors of climatic changes on the Earth is the increase in the concentration of carbon dioxide in the Earth's atmosphere. As the volume of industrial production in Russia increases, the exhausts of carbon dioxide into the atmosphere will soon reach such high values that there will arise a problem of reducing the exhausts in accordance with the Kyoto protocol. Various technologies of carbon-dioxide utilization are currently proposed. A promising method is gas conversion into a gas-hydrate state and its storage at the ocean bottom at low temperatures and high static pressures [1–5]. One important parameter that characterizes the cost efficiency of this method is the rate of formation of the carbon-dioxide hydrate. There are various methods of intensification of the process of gas hydration: spraying of a jet saturated by a gas into fine droplets in a gas atmosphere [6–8], intense mixing of water saturated by a gas dissolved there [7, 9, 10], vibrational effect on the liquid saturated by a gas [11], ultrasonic action on the medium [12], etc. The main drawback of these methods is the low rate of formation of gas hydrates and, as a consequence, low efficiency of facilities with the operation principle based on these methods.

Dontsov et al. [13] proposed a new shock-wave method of intensification of formation of gas hydrates. It was shown that the main mechanism that ensures intensification of the hydrate-formation process is the fragmentation of gas bubbles in a shock wave. The processes of dissolution and hydrate formation behind a moderate-amplitude shock wave in water with Freon-12 bubbles at atmospheric static pressure were studied in experiments in [14, 15]. A theoretical model of hydrate formation in a gas–liquid medium behind a shock wave with a stepwise profile was proposed. Fragmentation of gas bubbles, dissolution, and hydrate formation behind a shock wave in water with carbon-dioxide bubbles were studied in experiments with different initial static pressures in [16]. An increase in static pressure in the gas–liquid medium was demonstrated to reduce the relative shock-wave amplitude responsible for the development of the Kelvin–Helmholtz instability and fragmentation of bubbles into small gaseous inclusions behind the shock-wave front. An increase in static pressure in the medium with an unchanged relative amplitude of the wave was shown to enhance the rates of hydrate formation and dissolution of the gas in the liquid.

The present paper describes an experimental study of the processes of dissolution and hydrate formation behind a moderate-amplitude shock wave in water with gas bubbles (mixture of nitrogen and carbon dioxide) with different initial static pressures in the medium and concentrations of carbon dioxide in the bubbles.

Kutateladze Institute of Thermophysics, Siberian Division, Russian Academy of Sciences, Novosibirsk 630090; dontsov@itp.nsc.ru. Translated from Prikladnaya Mekhanika i Tekhnicheskaya Fizika, Vol. 50, No. 2, pp. 178–187, March–April, 2009. Original article submitted September 4, 2007; revision submitted December 7, 2007.

The experiments were performed in a shock-tube-type facility. The test section was a vertical thick-walled steel tube 1.5 m long; the inner diameter of the tube was 53 mm; the bottom end of the tube was bounded by a solid wall. The test section was filled by tap water under vacuum, which allowed us to avoid air bubbles in water. Gas bubbles were inserted in the lower part of the test section through holes 0.6 mm in diameter distributed over the test-section perimeter. The gas phase used was mixtures of nitrogen and carbon dioxide with different concentrations. Such a method of gas insertion ensures a rather high volume content of the gas. The mean bubble radius varied from 2 to 3 mm. The working liquid was tap water saturated by the gas mixture to an equilibrium state corresponding to the initial conditions (temperature and static pressure). The static pressure in the gas–liquid medium was varied from 0.5 to 1.3 MPa. A necessary static pressure in the medium was maintained by an electromagnetic valve controlled by a strain-gauge transducer mounted in the test section. The test section was thermostated by pumping a cooling liquid between the outer wall and the test-section jacket. The outer surface of the jacket was covered by a heat-insulating material. A thermostat and a cooling machine were used for pumping the cooling liquid. The liquid temperature in the test section was measured by two thermocouples placed in the top and bottom parts of the test section. The experiments were performed at an ambient temperature $T = 10$ and 1°C. The initial gas content φ_0 averaged over the test-section length was calculated on the basis of the liquid column height in the test section after insertion of gas bubbles. The bubble size was determined from the photographs taken by a digital camera equipped with additional optical devices through an optical window in the upper part of the test section.

Stepwise pressure waves were generated by breakdown of a diaphragm dividing the high-pressure chamber 2 m long and the test section. When the diaphragm was replaced, the test section was closed by a ball valve, which allowed us to avoid depressurization and degassing of the liquid. The ball valve with the diameter equal to the inner diameter of the test section was located in the upper part. The pressure wave profiles were recorded by a pressure piezo-transducer and by a strain-gauge transducer located along the test section and flush-mounted with the inner wall. To measure the local profile of the gas content behind the moderate-amplitude shock wave, we manufactured a conductivity gauge in a non-electroconducting tube with a square cross section; the end faces of this tube had a circular cross section equal to the cross section of the test section. The electrodes of the conductivity gauge were flush-mounted with the inner wall of the square tube, which made it possible to generate a uniform electric field in the region of measurements. In addition, the gauge electrodes did not alter the flow of the medium behind the wave, and the gauge could measure the profiles of the gas content behind the waves with fairly large amplitudes. The conductivity gauge located in the upper part of the test section measured the volume gas content averaged over the cross-sectional area of the test section and a height of 20 mm. The characteristic time of averaging was determined by the time needed for the wave to pass through the gauge; its value was smaller than 0.2 msec. The distance between the pressure piezo-transducer and the conductivity gauge was 60 mm. The signals from the gauges were fed to an analog-to-digital converter and were processed on a computer.

The process of dissolution of gas bubbles (mixture of nitrogen and carbon dioxide) in water behind a stepwise shock wave was studied experimentally. The study of the behavior of nitrogen bubbles behind the shock wave in the gas–liquid medium showed that the volume fraction of nitrogen dissolved in water behind the wave front for the medium and wave parameters used (static pressure in the medium $P_0 = 0.5$–1.3 MPa, wave amplitude $\Delta P = 2$–3 MPa, initial volume content of the gas $\varphi_0 = 15$–20%, and $T = 1$–10°C) at $t = 9$ msec was within 10%.

Figure 1 shows the profiles of pressure (curves 1) and local volume content of the gas (curves 2) behind the shock-wave front at a static pressure $P_0 = 0.5$ MPa, medium temperature $T = 10$°C and different initial values of the volume concentration of carbon dioxide in the gas mixture n. As no hydrates are formed at this temperature ($T_{\text{cr}} = 10$°C is the critical temperature of hydration for carbon dioxide), the gas content in the liquid behind the shock wave is determined only by compressibilities of the gases and by the amount of dissolved carbon dioxide. The gas bubbles directly behind the shock wave are compressed adiabatically (curves 2) and become fragmented owing to the Kelvin–Helmholtz instability (see [16]). Fragmentation of the bubbles behind the wave front involves thermal relaxation of the gas in the bubbles; hence, the gas content is expected to decrease to values corresponding to isothermal compression of the bubbles in the shock wave (as for insoluble bubbles of nitrogen) (curves 3). The process of intense dissolution of carbon dioxide, however, leads to a more significant decrease in the gas content behind the shock wave. During the time interval under study, the bubbles of pure carbon dioxide become almost completely dissolved behind the wave front (see Fig. 1a). At the initial stage, the main contribution to dissolution

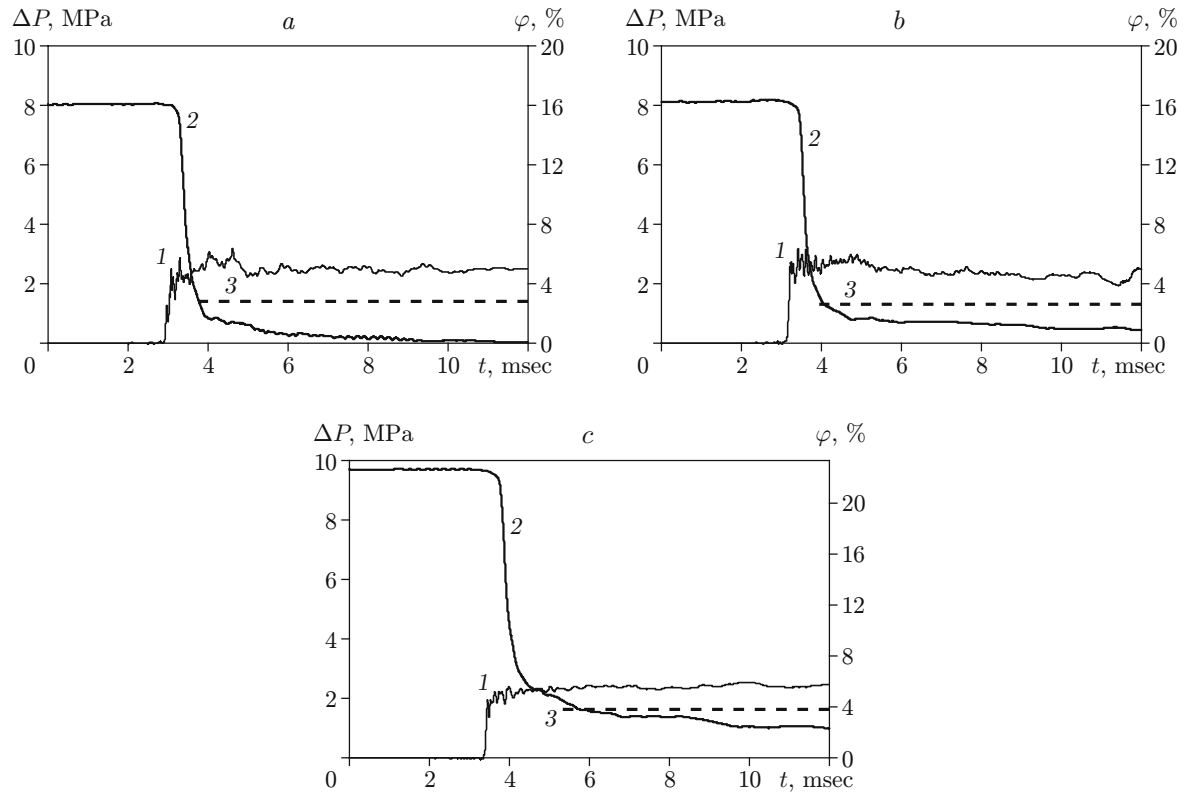

Fig. 1. Profiles of pressure (1), volume content of the gas (2), and volume content of the gas after isothermal compression of bubbles (3) in the shock wave with gas dissolution ($P_0 = 0.5$ MPa and $T = 10°$C): (a) $\Delta P = 2.45$ MPa, $\varphi_0 = 16.1\%$, and $n = 100\%$; (b) $\Delta P = 2.64$ MPa, $\varphi_0 = 16.2\%$, and $n = 55\%$; (c) $\Delta P = 2.47$ MPa, $\varphi_0 = 22.25\%$, and $n = 25\%$.

is made by convective diffusion caused by the relative motion of the gas bubbles in the liquid behind the shock-wave front. This time period is determined by the time of fragmentation of the gas bubbles and by the time of equalization of velocities of the gas and liquid phases. At higher times, the dissolution is caused by molecular diffusion of the gas into the liquid. Moreover, owing to fragmentation of the gas bubbles into small inclusions, intense mixing of the liquid occurs in the vicinity of the bubble, which also contributes to the process of gas dissolution.

A comparison of the experimentally measured profiles of the gas content (curves 2 in Fig. 1) with similar profiles in the case of isothermal compression of the gas bubbles behind shock waves of similar amplitudes (curves 3 in Fig. 1) for different concentrations of carbon dioxide in the bubbles allows us to conclude that addition of an insoluble (or weakly soluble) gas (nitrogen) leads to an increase in the gas content behind the shock wave. Nevertheless, a comparison of the volume concentrations of the dissolved gas at $t = 9$ msec in Figs. 1a to 1c shows that these values correspond to the initial values of the volume concentration of carbon dioxide in the bubbles (within the error of measurement of the gas-content profile). Thus, the presence of an insoluble gas in the bubble exerts almost no effect on the dissolution process, whereas even small additives of a non-absorbable gas in the case of absorption (or condensation) lead to substantial deceleration of the process because the interface between the phases becomes blocked by the non-absorbable gas [17]. The blockage of the interface by the non-absorbable gas is caused by the presence of a convective flux of the absorbable and non-absorbable gases toward the interface. In the examined problem of dissolution of the bubbles of a mixture of gases in a liquid, the process is determined by the dissolution kinetics and by the rate of removal of the dissolved gas from the interface to the liquid. The time of equalization of the carbon-dioxide concentration in the bubble τ_d is much smaller than the time of dissolution. Indeed, for the medium parameters corresponding to Fig. 1, we obtain $\tau_d = R^2/(\pi^2 D) < 0.5$ msec (R is the characteristic radius of gaseous inclusions of the fragmented bubble and D is the diffusion coefficient of carbon dioxide in nitrogen). In the course of dissolution of the bubbles of the gas mixture, carbon dioxide has a sufficient

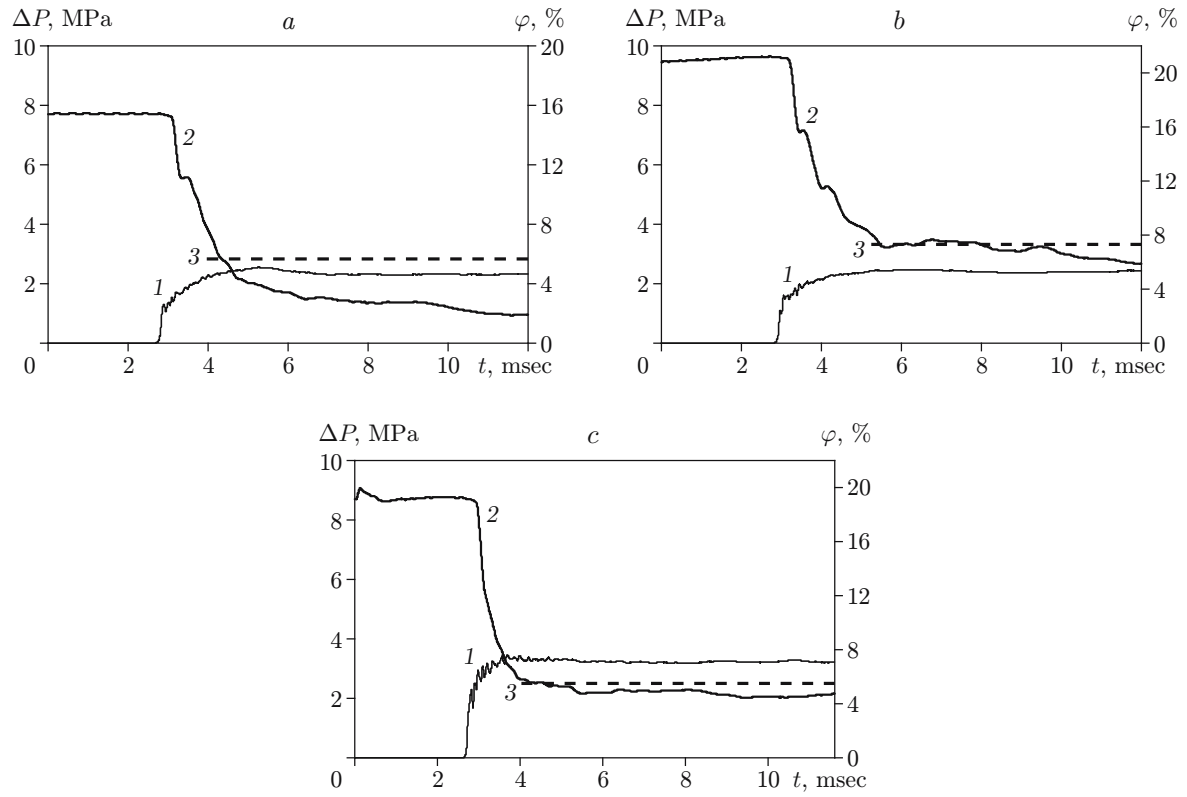

Fig. 2. Profiles of pressure (1), volume content of the gas (2), and volume content of the gas after isothermal compression of bubbles (3) in the shock wave with gas dissolution ($P_0 = 1.3$ MPa and $T = 10°$C): (a) $\Delta P = 2.3$ MPa, $\varphi_0 = 15.5\%$, and $n = 100\%$; (b) $\Delta P = 2.45$ MPa, $\varphi_0 = 21.1\%$, and $n = 25\%$; (c) $\Delta P = 3.2$ MPa, $\varphi_0 = 19.1\%$, and $n = 25\%$.

time to approach the interface, and nitrogen has a sufficient time to move away from the interface, the concentration of carbon dioxide in the bubble becomes equalized, and the dissolution process does not become decelerated.

Note that the non-coincidence of the fronts of the pressure wave and the volume content of the gas in Fig. 1 is caused by consecutive locations of the gauges in the shock tube.

Figure 2 shows the profiles of pressure (curves 1) and local volume content of the gas (curves 2) behind the shock-wave front for a static pressure $P_0 = 1.3$ MPa, temperature of the medium $T = 10°$C, and different initial values of the volume concentration of carbon dioxide in the gas mixture n. At increase in the static pressure P_0 in the medium for similar absolute values of the wave amplitude ΔP leads to a longer time of bubble fragmentation behind the wave front, a longer time of thermal relaxation of the gas in the bubbles, and, which is more important, a lower rate of carbon-dioxide dissolution in water (cf. Figs. 1a and 2a). The gas is completely dissolved at the examined times in the case with $P_0 = 0.5$ MPa (see Fig. 1a); in the case with $P_0 = 1.3$ MPa (see Fig. 2a), however, slightly more than half of the volume of carbon dioxide is dissolved. The main reason is a lower relative velocity of the gas bubbles behind the wave front and a greater size of gaseous inclusions [16].

Addition of a gas that is insoluble in water (nitrogen) to the bubbles at a static pressure $P_0 = 1.3$ MPa and a constant wave amplitude leads to almost complete termination of carbon-dioxide dissolution (see Fig. 2b). Thus, the presence of an insoluble gas in the bubble with increasing static pressure affects the dissolution process, which is attributed to the influence of equalization of the carbon-dioxide concentration in the bubble. As the static pressure increases, the size of the fragmented bubbles increases and the diffusion coefficient in the gas phase linearly decreases. The time of equalization of the carbon-dioxide concentration in the bubble τ_d (see Fig. 2b) is several milliseconds, which is comparable with the dissolution time.

As the shock-wave amplitude increases, the size of the fragmented bubbles and the time of equalization of the carbon-dioxide concentration in the bubbles decrease, which reduces the influence of the gas insoluble in the bubbles and enhances the solubility (see Fig. 2c).

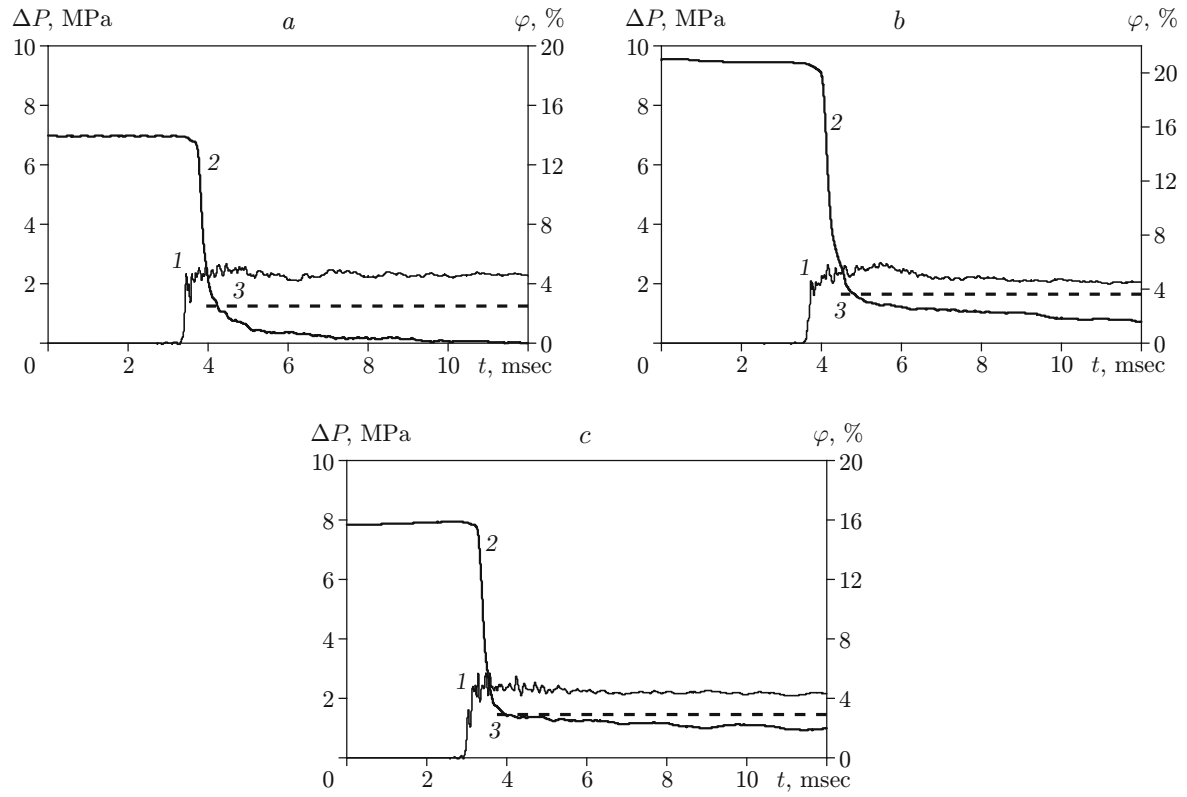

Fig. 3. Profiles of pressure (1), volume content of the gas (2), and volume content of the gas after isothermal compression of bubbles (3) in the shock wave with gas dissolution and hydrate formation ($P_0 = 0.5$ MPa and $T = 1°$C): (a) $\Delta P = 2.3$ MPa, $\varphi_0 = 13.9\%$, and $n = 100\%$; (b) $\Delta P = 2.35$ MPa, $\varphi_0 = 20.7\%$, and $n = 55\%$; (c) $\Delta P = 2.2$ MPa, $\varphi_0 = 15.6\%$, and $n = 25\%$.

Let us consider the process of carbon-dioxide hydrate formation in bubbles composed of a mixture of nitrogen and carbon dioxide in water behind a stepwise shock wave at a medium temperature $T = 1°$C. This temperature corresponds to an equilibrium pressure $P_e \approx 1.35$ MPa at which the carbon-dioxide hydrate is formed [18]. In this case, hydrate formation is possible in a gas–liquid medium behind a high-amplitude shock wave. Note that the degree of solubility of carbon dioxide in water increases by 50% as the medium temperature changes from $T = 10°$C to $T = 1°$C. Figure 3 shows the profiles of pressure (curves 1) and local volume content of the gas (curves 2) behind the shock-wave front for a static pressure $P_0 = 0.5$ MPa, medium temperature $T = 1°$C, and different initial volume concentrations of carbon dioxide in the gas mixture n. As was shown in [16], in the case of bubbles consisting of pure carbon dioxide, the rate of hydrate formation behind the shock wave is approximately equal to the rate of dissolution of carbon dioxide in water behind the shock wave with a similar amplitude. Hence, the character of the dependence $\varphi(t)$ in Fig. 3a is changed owing to the joint influence of dissolution and hydrate formation. A comparison of the volume concentration of partly dissolved and partly hydrated carbon dioxide behind shock waves of similar amplitudes in Figs. 3a to 3c suggests that they correspond to the initial values of the volume concentration of carbon dioxide in the bubbles (within the error of measurement of the gas-content profile). Thus, the presence of an insoluble gas (nitrogen) in the bubble exerts practically no effect on the processes of dissolution and hydrate formation.

A comparison of the gas-content profiles in Fig. 3 and Fig. 1 for the corresponding initial concentrations of carbon dioxide in the bubbles shows that a decrease in the medium temperature does not enhance the rate of variation of the gas content caused by hydrate formation. The reason can be the formation of gas-hydrate particles on the interface, leading to reduction of the gas–liquid interface area and, correspondingly, to a lower rate of carbon-dioxide dissolution in water.

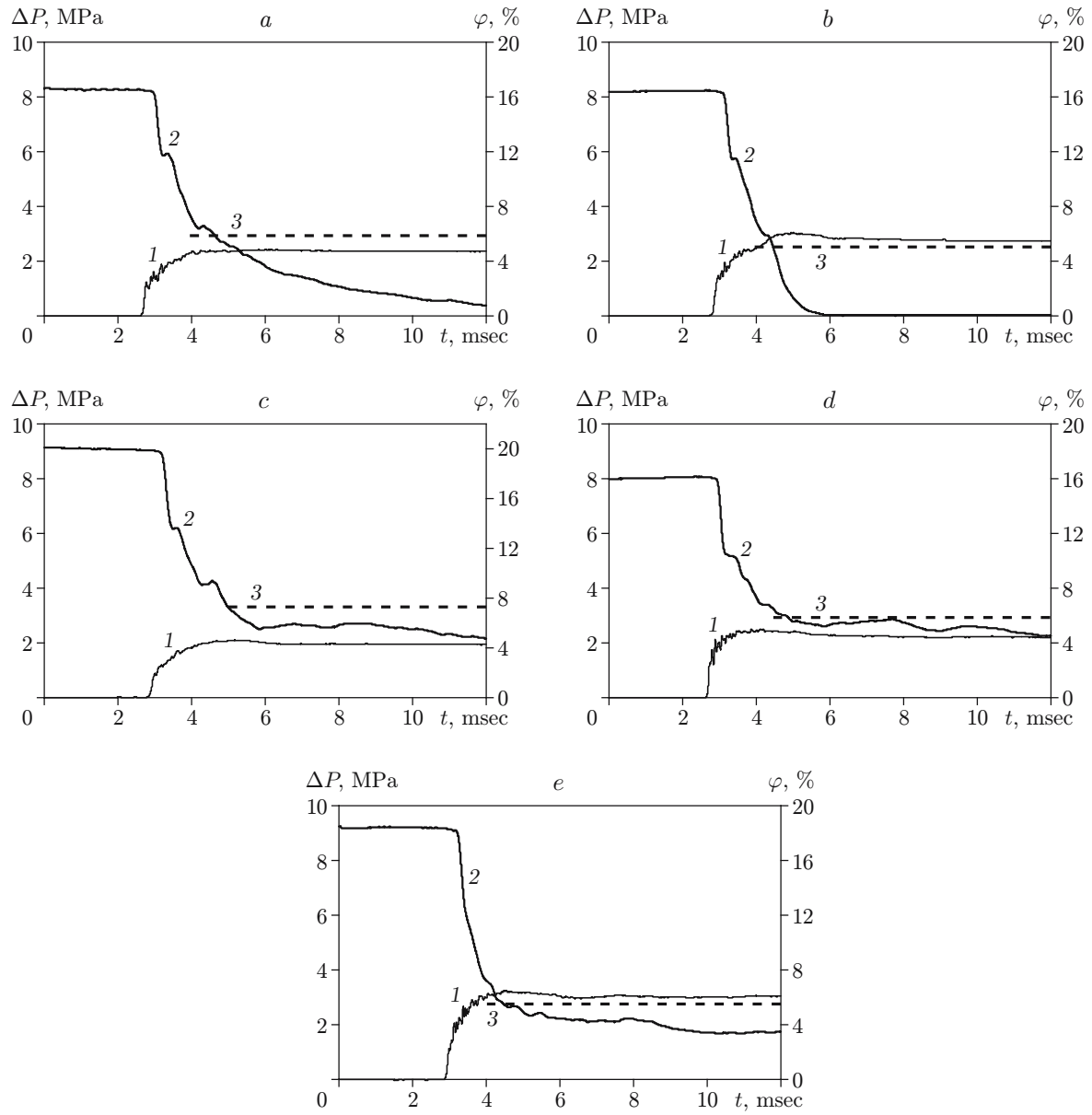

Fig. 4. Profiles of pressure (1), volume content of the gas (2), and volume content of the gas after isothermal compression of bubbles (3) in the shock wave with gas dissolution and hydrate formation ($P_0 = 1.3$ MPa and $T = 1°$C): (a) $\Delta P = 2.4$ MPa, $\varphi_0 = 16.5\%$, and $n = 100\%$; (b) $\Delta P = 2.85$ MPa, $\varphi_0 = 16.3\%$, and $n = 100\%$; (c) $\Delta P = 2.35$ MPa, $\varphi_0 = 20.2\%$, and $n = 55\%$; (d) $\Delta P = 2.3$ MPa, $\varphi_0 = 16.1\%$, and $n = 25\%$; (e) $\Delta P = 3.0$ MPa, $\varphi_0 = 18.4\%$, and $n = 55\%$.

Figure 4 shows the profiles of pressure (curves 1) and local volume content of the gas (curves 2) behind the shock-wave front for a static pressure $P_0 = 1.3$ MPa, medium temperature $T = 1°$C, and different initial volume concentrations of carbon dioxide in the gas mixture n. Figures 4a and 4b show the profiles of pressure and volume content of the gas in water with bubbles containing pure carbon dioxide for different wave amplitudes. It is seen that the decrease in the gas content caused by carbon-dioxide dissolution and hydrate formation substantially depends on the shock-wave amplitude. A 20% increase in amplitude leads to a several-fold decrease in the total time of reactions (dissolution and hydrate formation). The reason is that some part of the gas bubbles behind the shock wave becomes fragmented into small gaseous inclusions in the case of comparatively low wave amplitudes, whereas the other part of the bubbles remains in larger gaseous inclusions [16], which substantially delays the processes of hydrate formation and dissolution (Fig. 4a).

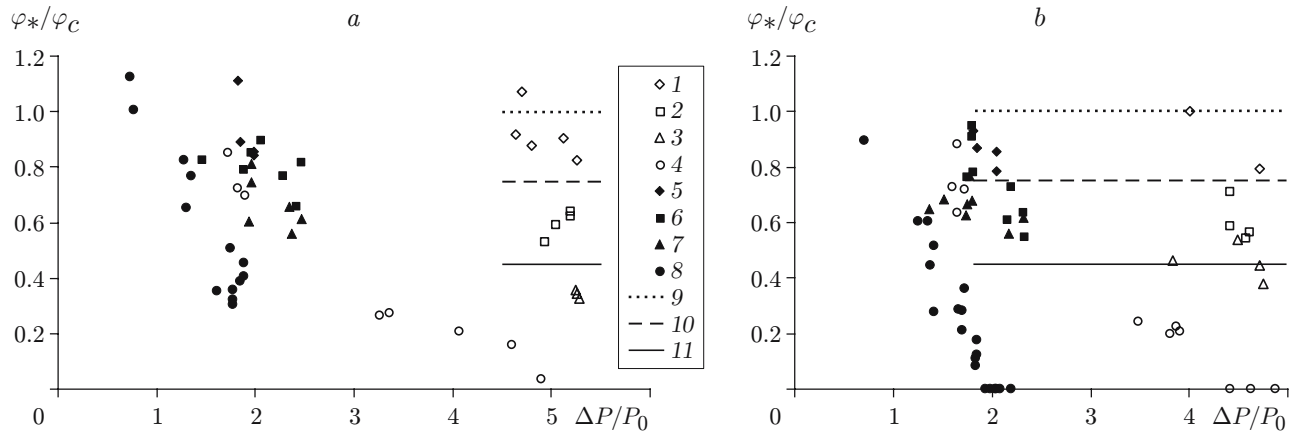

Fig. 5. Relative volume content of the gas ($t = 9$ msec) behind the shock-wave front versus the wave amplitude: $T = 10$ (a) and $T = 1^\circ$C (b); points 1–4 refer to $P_0 = 0.5$ MPa and $n = 0$ (1), 25 (2), 55 (3), and 100 (4); points 5–8 refer to $P_0 = 1.3$ MPa and $n = 0$ (5), 25 (6), 55 (7), and 100% (8); curve 9 shows the data for $\varphi_*/\varphi_c = 1$; curve 10 corresponds to complete dissolution (hydration) of carbon dioxide in bubbles with a concentration $n = 25\%$ ($\varphi_*/\varphi_c = 0.75$); curve 11 corresponds to complete dissolution (hydration) of carbon dioxide in bubbles with a concentration $n = 55\%$ ($\varphi_*/\varphi_c = 0.45$).

Addition of a gas insoluble in water (nitrogen) to the bubbles at a static pressure $P_0 = 1.3$ MPa and a constant wave amplitude leads to significant deceleration of the processes of hydrate formation and dissolution of carbon dioxide (Figs. 4a, 4c, and 4d). Almost 90% of carbon dioxide become hydrated and dissolved behind the wave front during the examined time interval in the case of the bubbles with a carbon-dioxide concentration $n = 100\%$ (Fig. 4a), whereas the corresponding value for the gas–liquid medium with $n = 55\%$ is only 60% (Fig. 4c). As was noted above (in studying the process of carbon-dioxide dissolution), the reason is equalization of the carbon-dioxide concentration in the bubble. In addition, the diffusion coefficient in the gas phase depends not only on the pressure in the medium, but also on the medium temperature. Therefore, the time of equalization of the carbon-dioxide concentration in the bubble τ_d increases with decreasing temperature, which results in a greater effect of the inert gas on the process and, correspondingly, in lower rates of dissolution and hydrate formation.

An increase in the shock-wave amplitude in the liquid with bubbles of a mixture of gases with identical concentrations leads, on one hand, to an increase in pressure behind the wave front and, on the other hand, to a decrease in size of fragmented bubbles in the medium. Owing to the increase in pressure, the diffusion coefficient in the gas phase decreases and, correspondingly, the time of equalization of the carbon-dioxide concentration in the bubbles increases. Vice versa, a decrease in size of fragmented bubbles in the medium leads to a shorter time of equalization of the carbon-dioxide concentration in the bubbles. As τ_d experiences a stronger dependence on the bubble radius, the increase in the shock-wave amplitude reduces the effect of the insoluble gas in the bubbles on hydrate formation and dissolution; correspondingly, the rates of these processes increase (Figs. 4c and 4e).

Figure 5 shows the experimental dependences of the relative volume content of the gas at $t = 9$ msec behind the shock-wave front on the wave amplitude for different initial concentrations of carbon dioxide in the bubbles, temperatures, and initial static pressures in the gas–liquid medium (φ_* is the volume content of the gas measured behind the shock-wave front at the time $t = 9$ msec and φ_c is the calculated value corresponding to isothermal compression of bubbles in the shock wave). The experimental points in Fig. 5a refer to the medium temperature $T = 10^\circ$C equal to the critical temperature of hydrate formation; hence, the change in the gas content is caused only by gas solubility. The points in Fig. 5b refer to the process of dissolution and hydrate formation behind the shock wave. It should be noted that the solubility of nitrogen in water is almost 50 times lower than the solubility of carbon dioxide at an identical temperature; nevertheless, approximately 10% of nitrogen contained in the bubbles become dissolved in water under the examined parameters of the medium and wave (points 1 and curve 9 in Fig. 5). A comparison of the experimental points 8 (and also points 4) for the bubbles of pure carbon dioxide ($n = 100\%$) in Figs. 5a and 5b shows that a decrease in the medium temperature reduces the relative volume content of the gas for a given wave amplitude. The reason is the increase in solubility of carbon dioxide with decreasing temperature

of the medium and the influence of the process of hydrate formation [16]. At a temperature $T = 1°C$ (Fig. 5b), the processes of hydrate formation in the medium start at the wave amplitude $\Delta P/P_0 \approx 2$ for $P_0 = 1.3$ MPa and $\Delta P/P_0 \approx 4$ for $P_0 = 0.5$ MPa. It is rather difficult to determine the fraction of the hydrated gas in the course of dissolution and hydrate formation by comparing the points in Figs. 5a and 5b, because the formation of gas-hydrate particles on the interface reduces the area of the gas–liquid interface, which decreases the rate of dissolution of carbon dioxide in water. The processes of dissolution and hydrate formation cannot be separated in time either because of similar reaction rates.

Let us determine the effect of the presence of a non-hydrated gas weakly soluble in water (nitrogen) in gas bubbles. As was noted above, the presence of a non-reacting gas in the bubbles does not affect the examined processes at a static pressure $P_0 = 0.5$ MPa. Indeed, points 2 are fairly close to curve 10 corresponding to complete dissolution (hydration) of carbon dioxide in bubbles with a concentration $n = 25\%$, and points 3 are close to curve 11 (Fig. 5). It should be noted that the deviation of the experimental points from the calculated curves is caused by the neglect of partial dissolution of nitrogen in the bubbles. As the static pressure increases ($P_0 = 1.3$ MPa), the experimental points 7 for bubbles with a concentration of carbon dioxide $n = 55\%$ become substantially deviated from curve 11, which is attributed to the influence of equalization of the carbon-dioxide concentration in the bubbles on dissolution and hydrate formation.

Thus, the processes of dissolution and hydrate formation of carbon dioxide behind the front of a moderate-amplitude shock wave in water with gas bubbles (mixture of nitrogen and carbon dioxide) are studied in experiments with different initial static pressures and carbon-dioxide concentrations. For $P_0 = 0.5$ MPa, the presence of a non-reacting gas (nitrogen) in the bubbles is demonstrated to exert almost no effect on carbon-dioxide dissolution in water and hydrate formation, whereas even small additives of a non-absorbable gas in the case of absorption (or condensation) lead to substantial deceleration of the process because the interface between the phases becomes blocked by the non-absorbable gas. At a static pressure $P_0 = 1.3$ MPa, addition of nitrogen to bubbles containing carbon dioxide leads to substantial deceleration of the processes of carbon-dioxide dissolution and hydrate formation.

This work was supported by the Russian Foundation for Basic Research (Grant No. 06-08-00657).

REFERENCES

1. N. Handa and T. Oshumi (eds.), *Direct Ocean Disposal of Carbon Dioxide*, Terrapub., Tokyo (1995).
2. V. Anderson, S. Woodhouse, O. Fr. Graff, and J. S. Gudmundson, "Hydrates for deep ocean storage of CO_2," in: *Proc. of the 5th Int. Conf. on Gas Hydrates* (Trondheim, Norway, June 13–16, 2005), S. n., Trondheim (2005), P. ref. 4006, pp. 1135–1139.
3. S. Tanaka, F. Maruyama, O. Takano, et al., "Experimental study on CO_2 storage and sequestration in form of hydrate pellets," in: *Proc. of the 5th Int. Conf. on Gas Hydrates* (Trondheim, Norway, June 13–16, 2005), S. n., Trondheim (2005), P. ref. 4028, pp. 1314–1319.
4. S. Tanaka, O. Takano, K. Uchida, et al., "Gas hydrate formation technology using low-temperature and low-pressure conditions. Part 2. Study on application to CO_2 separation with a bench plant," in: *Proc. of the 5th Int. Conf. on Gas Hydrates* (Trondheim, Norway, June 13–16, 2005), S. n., Trondheim (2005), P. ref. 4031, pp. 1332–1339.
5. M. Ota, M. Seko, and H. Endou, "Gas separation process of carbon dioxide fro mixed gases by hydrate production," in: *Proc. of the 5th Int. Conf. on Gas Hydrates* (Trondheim, Norway, June 13–16, 2005), S. n., Trondheim (2005), P. ref. 4032, pp. 1340–1343.
6. R. Ohmura, S. Kashiwazaki, S. Shiota, et al., "Structure-1 and structure-2 hydrate formation using water spraying," in: *Proc. of the 4th Int. Conf. on Gas Hydrates* (Yakohama, Japan, May 19–23, 2002), S. n., Yakohama (2002), pp. 1049–1054.
7. K. Miyata, T. Okui, H. Hirayama, et al., "A challenge to high-rate industrial production of methane hydrate," in: *Proc. of the 4th Int. Conf. on Gas Hydrates* (Yakohama, Japan, May 19–23, 2002), S. n., Yakohama (2002), pp. 1031–1035.
8. I. S. Gudmundson, "Method of obtaining gas hydrates for transportation and storage," RF Patent No. 2200727, C 07 C 5/02, No. 97112086/06, Appl. 07.02.1997, Publ. 03.20.2003, Bul. No. 8.

9. V. S. Yakushev, "Method of extraction and transportation of natural gas from gas and gas-hydrate sea-based deposits — flowers and bees," RF Patent No. 2198285, E 21 B 43/01, No. 98113838/03, Appl. 07.13.1998, Publ. 02.10.2003, Bul. No. 4.
10. H. Tajima, A. Yamasaki, F. Kiyono, et al., "Continuous gas hydrate formation process by static mixing of fluids," in: *Proc. of the 5th Int. Conf. on Gas Hydrates* (Trondheim, Norway, June 13–16, 2005), S. n., Trondheim (2005), P. ref. 1010, pp. 75–80.
11. K. B. Komissarov and V. A. Finochenko, "Facility for obtaining gas hydrates," RF Patent No. 2045718, F 25 D 3/12, No. 5044706/13, Appl. 05.29.1992, Publ. 10.10.1995, Bul. No. 28.
12. Y. Kozo, F. Tetsuro, K. Takahiro, and K. Yuichi, "Production method for gas hydrates and device for producing same," Patent No. 2347938 A GB, C 07 C7/152, No. 0006039.2, Publ. 20.09.2000.
13. V. E. Dontsov, V. E. Nakoryakov, and L. S. Chernoi, "Method of obtaining gas hydrates," RF Patent No. 2270053, B 01 F 3/04, No. 2003133051/15, Appl. 11.11.2003, Publ. 02.20.2006, Bul. No. 5.
14. V. E. Dontsov, V. E. Nakoryakov, and A. A. Chernov, "Formation of gas hydrates in a gas–liquid mixture behind a shock wave," *Dokl. Ross. Akad. Nauk*, **411**, No. 2, 190–193 (2006).
15. V. E. Dontsov, V. E. Nakoryakov, and A. A. Chernov, "Shock waves in water with Freon-12 bubbles and formation of gas hydrates," *J. Appl. Mech. Tech. Phys.*, **48**, No. 3, 346–360 (2007).
16. V. E. Dontsov, A. A. Chernov, and E. V. Dontsov, "Shock waves and hydrate formation of carbon dioxide with an elevated initial pressure in a gas–liquid medium," *Teplofiz. Aéromekh.*, **14**, No. 1, 23–46 (2007).
17. H. M. Habib and B. D. Wood, "Simultaneous heat and mass transfer in film absorption with the presence of non-absorbable gases," *Trans. ASME*, **123**, 984–989 (2001).
18. Y. F. Makogon, *Gas Hydrates, Preventing Their Formation, and Their Applications* [in Russian], Nedra, Moscow (1985).